

# 2D Nanosilicates Loaded with Proangiogenic Factors Stimulate Endothelial Sprouting

David W. Howell, Charles W. Peak, Kayla J. Bayless,\* and Akhilesh K. Gaharwar\*

Therapeutic angiogenesis remains a major clinical challenge due to lack of biomaterials to sequester and deliver proangiogenic therapeutics. Here, 2D nanosilicates are introduced as a platform technology to sequester and deliver a multitude of proangiogenic growth factors to stimulate angiogenesis. The high surface area and charged characteristics of nanosilicates prolong release of proangiogenic molecules. Interestingly, nanosilicates can maintain bioavailability compared to exogenously delivered biomolecules. Incorporation of therapeutics-loaded nanosilicates within collagen hydrogels stimulates endothelial cell invasion in a 3D *in vitro* models of angiogenesis. The results show that endothelial cell invasion is controlled predominately by the type of growth factors conjugated to the nanosilicates. Overall, this work illustrates the importance of nanosilicates as a platform technology to noncovalently conjugate proangiogenic therapeutics to direct angiogenesis.

## 1. Introduction

Angiogenesis is a dynamic, multistep process that requires endothelial cells to undergo biochemical, morphological, and biophysical changes to accomplish basement membrane degradation, sprout initiation, proliferation, migration, lumen formation, and stabilization.<sup>[1]</sup> A range of rationally designed approaches are proposed to engineer angiogenic biomaterials.<sup>[2]</sup> However, therapeutic angiogenesis remains a major clinical challenge and only a few approaches have reached the

market for wound-healing applications.<sup>[2]</sup> Thus, there is an unmet clinical need to develop new approaches to deliver proangiogenic therapeutics. Here, we introduce 2D nanosilicates (nSi) as a platform technology to sequester and deliver multiple proangiogenic growth factors to stimulate angiogenesis. These 2D nanosilicates are discotic, charged nanoparticles that are reported as 30–50 nm in diameter and 1–2 nm in thickness.<sup>[3,4]</sup> Due to unique structural arrangements, the surface of nanosilicates is negatively charged and the edge is positively charged. We propose to use the high surface area and charged characteristics of nanosilicates for sustained and prolonged delivery of proangiogenic molecules.

Sequestering proangiogenic factors within biomaterials can be used to pattern and direct angiogenesis in tissue engineered scaffolds. Proangiogenic factors, such as vascular endothelial growth factor (VEGF), fibroblast growth factor (FGF), and platelet derived growth factor (PDGF), have been used to stimulate endothelial cells to form capillary networks in synthetic scaffolds.<sup>[5,6]</sup> However, our inability to accurately pattern angiogenic factors in a scaffold is a critical limiting step to engineer vascularized tissues.<sup>[7]</sup> If these proangiogenic factors are randomly distributed within a tissue engineered scaffold, this could affect the normal growth and activities of nonvascular cells. Although techniques such as covalent crosslinking can solve this problem by appending functional proteins to the materials, crosslinking agents have potential to also inactivate the tethered protein or remain embedded in the materials, rendering them toxic to cells.<sup>[8]</sup>

A variety of polymeric, metallic, and ceramic nanomaterials are being investigated to design angiogenic biomaterials.<sup>[9]</sup> Specifically, there is a need to design and develop new nanocomposite biomaterials that deliver specific molecular cues and direct vascular cell adhesion, differentiation, migration, and extracellular matrix deposition.<sup>[10]</sup> However, most of these nanoengineered biomaterials are not able to sequester biomolecules for prolonged durations. Extracellular responses to growth factors *in vitro* are dependent on exposure to adequate concentrations<sup>[11]</sup> while *in vivo*, overexpression of proangiogenic factors can result in aberrant angiogenesis<sup>[12]</sup> and enhanced angiogenic responses within tumors.<sup>[13]</sup> Therefore, sustained and prolonged release of physiologically relevant dose of biomolecules can overcome these problems.


We propose to use 2D nanosilicates to sequester multiple growth factors and delay their release to direct angiogenesis.

Dr. D. W. Howell, Prof. K. J. Bayless  
Department of Molecular and Cellular Medicine  
Texas A&M University Health Science Center  
College Station, TX 77843, USA  
E-mail: kbayless@medicine.tamhsc.edu

Dr. C. W. Peak, Prof. A. K. Gaharwar  
Biomedical Engineering  
Dwight Look College of Engineering  
Texas A&M University  
College Station, TX 77843, USA  
E-mail: gaharwar@tamu.edu

Prof. A. K. Gaharwar  
Material Science and Engineering  
Dwight Look College of Engineering  
Texas A&M University  
College Station, TX 77843, USA

Prof. A. K. Gaharwar  
Center for Remote Health Technologies and Systems  
Texas A&M University  
College Station, TX 77843, USA

 The ORCID identification number(s) for the author(s) of this article can be found under <https://doi.org/10.1002/adbi.201800092>.

DOI: 10.1002/adbi.201800092

Nanosilicate (Laponite XLG,  $\text{Na}^{+}_{0.7}[(\text{Mg}_{5.5}\text{Li}_{0.3})\text{Si}_8\text{O}_{20} \cdot (\text{OH})_4]^{-0.7}$ ) a hydrous sodium lithium magnesium silicate and its ionic dissociation products (magnesium, orthosilicic acid, and lithium) can be readily absorbed *in vivo* and have been shown to be biocompatible.<sup>[14]</sup> The complex phase diagram and presence of an electrical double layer permits therapeutic binding to the nanosilicates surface.<sup>[15,16]</sup> Establishing nanosilicates as a platform technology for sequestering and delivery of proangiogenic factors will have significant impact on designing next-generation of bioactive scaffolds. Previous work has reported singular delivery of either bone morphogenic protein-2 (BMP2) or VEGF using clay-based gels.<sup>[4,17]</sup> Similarly, other studies have delivered either dexamethasone or doxorubicin using nanosilicate-based biomaterials.<sup>[18,19]</sup> However, none of the earlier studies have shown delivery of multiple growth factors or biomolecules using nanosilicates or nanosilicate-based hydrogels.

The bioactivity of sequestered proangiogenic molecules can be determined using 3D invasion assays. 3D *in vitro* models of angiogenesis have emerged as reliable tools for studying different steps of angiogenesis,<sup>[5,20]</sup> along with a number of useful *in vivo* models.<sup>[21]</sup> These approaches have illuminated underlying mechanisms that control lumen formation<sup>[22,23]</sup> and endothelial cell sprouting.<sup>[5,22,24]</sup> Recently, we reported a straightforward and quantitative approach to investigate the bioactivity of proangiogenic factors using invasion assays,<sup>[25]</sup> which allow examination of the sprouting step of angiogenesis. Monolayers of endothelial cells penetrate 3D collagen matrices and form sprouting structures orthogonal to the monolayer. The activity of biomolecules can be determined by quantifying invasion distance and frequency.

After establishing nanosilicates as a therapeutic delivery platform, we have developed a collagen-based platform to promote angiogenesis. The presence of an electrical double layer permits therapeutic binding to and delayed release from nanosilicates.<sup>[16]</sup> Utilizing the ion exchange capacity of nanosilicates, multiple growth factors are incorporated into collagen-based hydrogels that can be injected into a localized site and thermogelled. We hypothesize that the incorporation of nanosilicates will provide enhanced growth factor retention and prolonged release of several growth factors to promote angiogenesis. The interactions mediated by nanosilicates have the potential to be broadly used as a growth factor delivery and release mechanism while not interfering with mechanical properties of samples. The proposed composite collagen and nanosilicate scaffolds further our understanding of this emerging class of biomaterials.

## 2. Results and Discussion

### 2.1. Nanosilicates for Growth Factor Delivery

Nanosilicates are disc-shaped particles 1–2 nm thick and 20–30 nm in diameter (Figure 1a). Nanosilicates form stable colloidal networks in aqueous solution releasing counter ions from the surface.<sup>[26]</sup> The displacement of counter ions from the nanosilicate surface enables conjugation of growth factors through ionic interactions (Figure 1a). Growth factors or protein were added with increasing amounts of pre-exfoliated

nanosilicates, mixed for 24 h, and centrifuged to separate nanosilicates/growth factor conjugate from media and unbound growth factor (Figure 1b). To confirm protein adsorption to nanosilicates, bovine serum albumin (FBS) ( $40 \text{ ng mL}^{-1}$ ) was used as a model protein. Dynamic light scattering (DLS) and zeta potential measurements confirmed that nanosilicates/albumin conjugation occurred. Loading of protein was confirmed by microBCA assay (Figure 1c). Addition of growth factor via hydrogen bonding and van der Waals interactions results in an increase in hydrodynamic diameter of nanosilicates. Growth factors were ionically exchanged with the sodium ion to stabilize the solution, but growth factors are much larger than sodium ions, resulting in a larger particle size. Additionally, the zeta potential shifts from  $-27 \pm 5 \text{ mV}$  (blank nanosilicates) to  $-24 \pm 0.3 \text{ mV}$  with the addition of growth factor suggesting that growth factor does not destabilize the nanosilicates. Release of protein/growth factor was measured via microBCA assay and suggests the protein can readily adsorb and desorb onto blank nanosilicates.

### 2.2. Functionalization of Nanosilicates with Proangiogenic Growth Factors

To understand the ability of growth factor-loaded nanosilicates to affect cell behavior, we used a 3D invasion assay (Figure 2a). In this study, we examined the effect of growth factor-loaded nanosilicates on the sprouting step of angiogenesis.<sup>[5,27,28]</sup> Specifically we selected three major proangiogenic proteins including VEGF, FGF, and PDGF. As a control, sphingosine 1-phosphate (S1P)<sup>[29]</sup> and growth factors (VEGF and bFGF) were included to stimulate the invasion of a monolayer of endothelial cells (ECs) into a basal 3D collagen matrix (Figure S1a, Supporting Information).<sup>[30]</sup> Endothelial cells subsequently penetrate the collagen matrices overnight and form sprouting structures orthogonal to the monolayer and exhibit a uniform response. Quantification of sprouting indicates that growth factors and S1P both promote invasion independently, but are most effective in combination (Figure S1b, Supporting Information). Similarly, the nanosilicates/growth factor conjugate and the excess media with growth factors were tested. A range of nanosilicates (0%, 0.005%, 0.015%, and 0.05% w/v) was used to determine the minimum concentration of nanosilicates necessary to adsorb sufficient growth factor to induce invasion. After 24 h, the invasion distance and frequency was examined (Figure 2b). Both media-depleted with growth factor and nanosilicates/growth factor conjugates showed invasion; however, minimal invasion is expected due to the presence of S1P (Figure S1, Supporting Information). Quantification of cell invasion numbers reveals two trends: the ability of depleted media to induce invasion decreases with increasing nanosilicates concentration and the number of invading cells increases with higher nanosilicates/growth factor conjugates (Figure 2c; similar symbols denote significance,  $p < 0.01$ ). The data suggest that a minimum concentration of 0.015% nanosilicates is required to adsorb growth factors that match the effect of exogenously administered growth factor. There is a strong correlation between the invasion number and the concentration of nanosilicates. As nanosilicate concentration increases, the

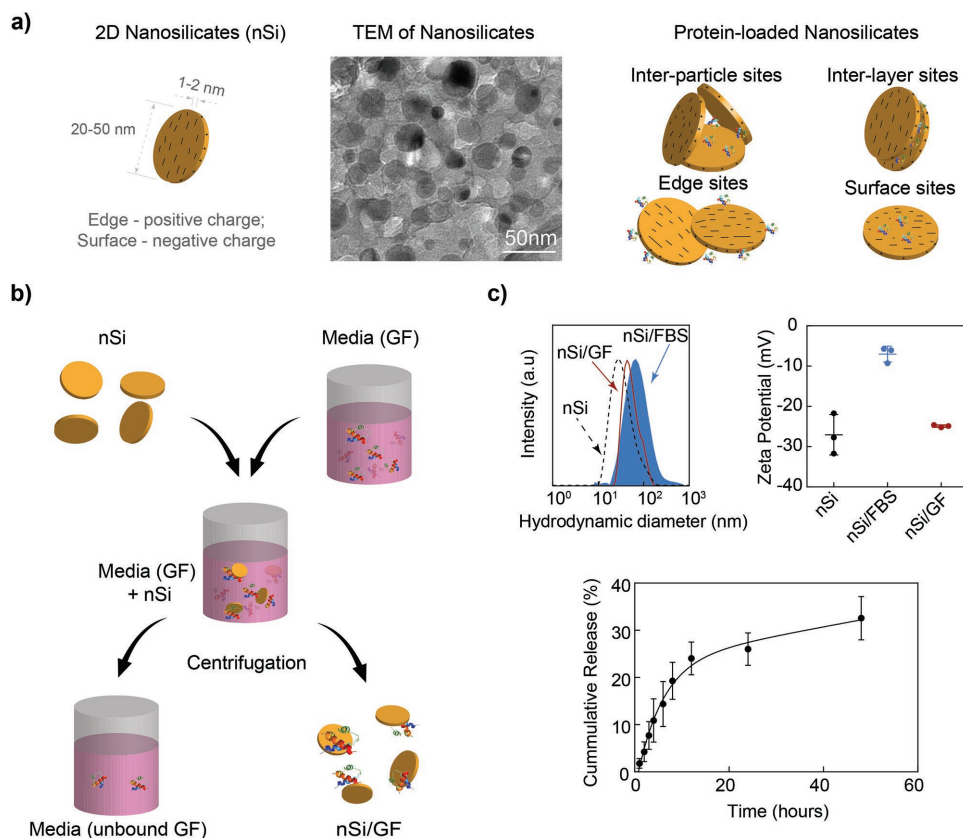


**Figure 1.** Nanosilicates sequester proangiogenic factors. a) TEM image of nanosilicate show diameter  $\approx 20\text{--}50$  nm (Laponite XLG). b) Sequestration of growth factor. Growth factors (VEGF and bFGF) were incubated with 0%, 0.005%, 0.015%, and 0.05% nanosilicate before mixtures were centrifuged to pellet the nanosilicate and the media (unbound GF) is added in endothelial invasion assays. The pelleted nanosilicate is resuspended and tested separately (GF-loaded nanosilicates). c) Sequestering of protein on nanosilicates results in increase in hydrodynamic diameter ( $n = 3$ ) and zeta potential ( $n = 3$ , mean  $\pm$  standard deviation). Release profile (as measured by microBCA assay) of FBS from nanosilicates fitted with nonlinear two-phase association ( $R^2 = 0.9108$ ) ( $n = 3$ , mean  $\pm$  standard deviation).

ability to adsorb growth factors when placed in media increases, suggesting that there is a minimum ratio between nanosilicates and growth factor. An increase in invasion with samples containing nanosilicates compared to exogenously delivered growth factors is hypothesized to occur since the growth factor can be released over time. The ability to replicate an established soluble growth factor model of invasion<sup>[25]</sup> suggests that nanosilicates/growth factor conjugates hold promise as an exogenous delivery vehicle.

### 2.3. Synthesis of Collagen-Nanosilicates Hydrogels

Bolus delivery of nanoparticles loaded with proangiogenic growth factors is not effective at directing angiogenesis. However, sequestering proangiogenic factors within collagen matrices can direct cell migration and angiogenesis. Here, we will evaluate the effect of nanosilicates on gelation kinetics and mechanical stability of collagen matrices. Collagen matrices are formed via polymerization with a neutral pH at 37 °C. Prior to matrix formation, the collagen solutions have fluid-like consistency. Shear rate dependence of viscosity for collagen and collagen/nanosilicates matrices were investigated using

continuous shear flow measurements. Shear-thinning behavior of matrices is observed as demonstrated with a decrease in viscosity over increasing shear rate (Figure 3a). Shear-thinning behavior is important for localization of the matrices after injection within the body.<sup>[31]</sup> Both collagen and collagen/nanosilicates exhibit shear-thinning behavior and the inclusion of nanosilicates (0.015%) did not influence the shear-thinning ability of collagen matrices. Temperature was precisely controlled at 37 °C using a Peltier plate during shear-thinning experiments suggesting collagen has not fully crosslinked and can be extruded through a needle to be delivered in precise locations while undergoing polymerization. Subsequent temperature ramp followed by a time sweep corroborates these conclusions (Figure 3b). Initially the storage modulus ( $G'$ ) is equal to or less than the loss modulus ( $G''$ ). With an increase in temperature from 25 to 37 °C a rapid increase in both  $G'$  and  $G''$  occurs with  $G'$  overtaking  $G''$ . Upon reaching physiological temperature (37 °C),  $G'$  is  $\approx 100$  Pa for both samples. This suggests that during matrix formation and curing that nanosilicates do not interfere with collagen fibril formation and that there is no difference in mechanical stability of the samples. Strain sweep suggests that samples containing nanosilicates have a storage modulus equal to those that do not contain nanosilicates. Further, nanosilicate samples

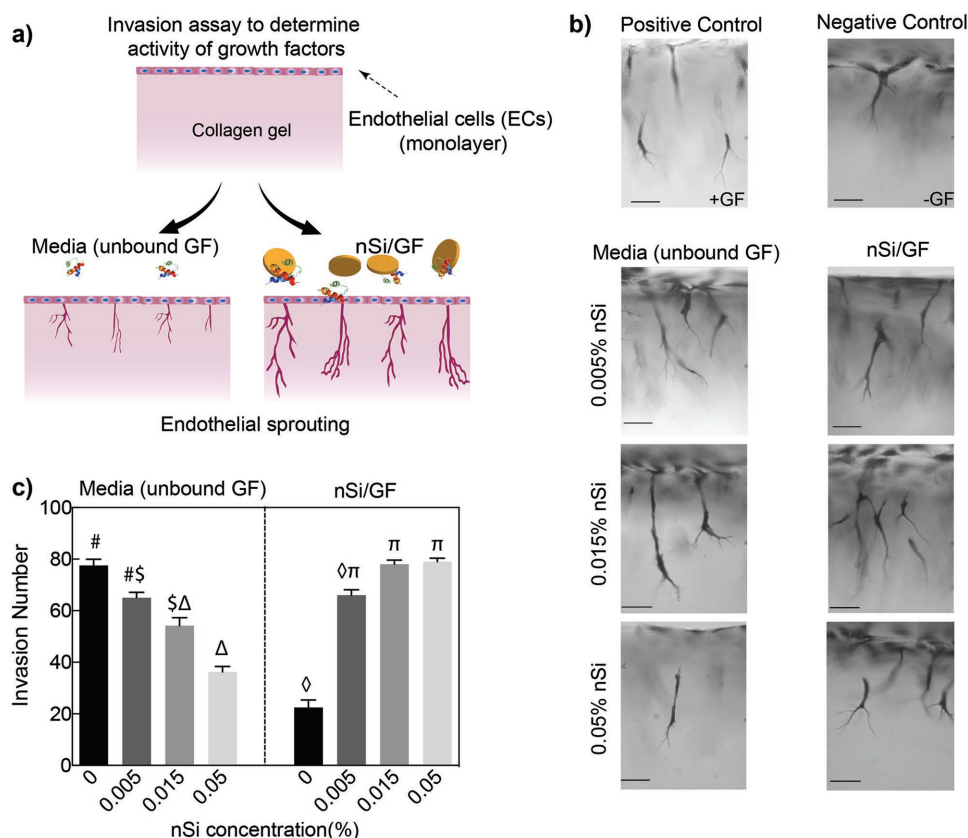


**Figure 2.** Nanosilicates sequester proangiogenic factors. a) Schematic showing in vitro assay to determine the ability of nanosilicate (nSi) to sequester growth factors. Images of each invasion condition show the response to GFs incubated with increasing amounts of nSi. b) The number of invading structures that form in response to depleted GF (Media (unbound GF)) and GF-loaded nanosilicate (nSi/GF) media (Scale bar = 50  $\mu\text{m}$ ). c) The number of invading structures that form in response to media depleted of GF (Media (unbound GF)) and GF-loaded onto nanosilicates (nSi/GF) ( $n = 3$ , mean  $\pm$  standard deviation). Significance was determined using analysis of variance with Tukey's post hoc test for multiple comparisons and multiplicity-adjusted  $P$ -values. Similar symbols denote a significant relationship,  $p < 0.01$ .

can withstand as much strain as those without (Figure 3c). These data suggest that collagen and collagen/nanosilicate matrices exhibit similar mechanical properties. Additionally, there is no frequency dependence in modulus (Figure 3d). Overall, these data suggest that nanosilicate addition at such low concentration (0.015%) does not increase the mechanical properties of collagen matrices.

#### 2.4. Sequestering Proangiogenic Growth Factors within Collagen/Nanosilicate Matrices

Nanosilicates can maintain growth factor bioavailability compared to exogenously delivered factors. However, nanosilicates must be incorporated into a stable matrix to prevent diffusion. Therefore, growth factors loaded onto nanosilicates to induce angiogenesis must be incorporated into a scaffold such as a collagen matrix. To fully develop a nanocomposite material, two main concerns surround nanoparticle use: cytocompatibility and matrix mechanics. Our earlier study showed that the  $\text{IC}_{50}$  value of nanosilicates to be above  $10^3 \mu\text{g mL}^{-1}$ .<sup>[32]</sup> Rheological analysis shows that nanosilicates do not alter mechanical behavior of collagen matrices. Together, there is strong

potential for nanosilicates to be used in collagen matrices solely as a growth factor delivery vehicle. To examine possible effects of nanosilicates in our 3D collagen invasion system, we used four different conditions in the 3D invasion system (Figure 4a): 1) collagen matrix with growth factors (VEGF, FGF) in the media (control); 2) collagen matrix with growth factors embedded in the matrix; 3) blank nanosilicate embedded in the collagen matrix with growth factors in the media; and 4) growth factor-loaded nanosilicate embedded in the collagen matrix. Both the number and distance of invading structures are critical components of assessing an angiogenic response and are dependent on mechanical stiffness of the matrix,<sup>[33]</sup> fluid shear stress,<sup>[28]</sup> and delivery of appropriate concentrations of angiogenic factors.<sup>[5]</sup> Our results support that nanosilicates alter the invasion number and distance by sequestering growth factors. This assay looks at invasion over a short duration (18 h) therefore, growth factors exogenously delivered in the media are taken up by more cells at the surface inducing a larger amount of invading cells but shorter invasion distance compared to when nanosilicates are included (Figure 4b; # denotes significant difference,  $p < 0.001$ ). The localization and sequestration of growth factors on the nanosilicates is responsible for these results. Growth factors appear to adsorb onto nanosilicates

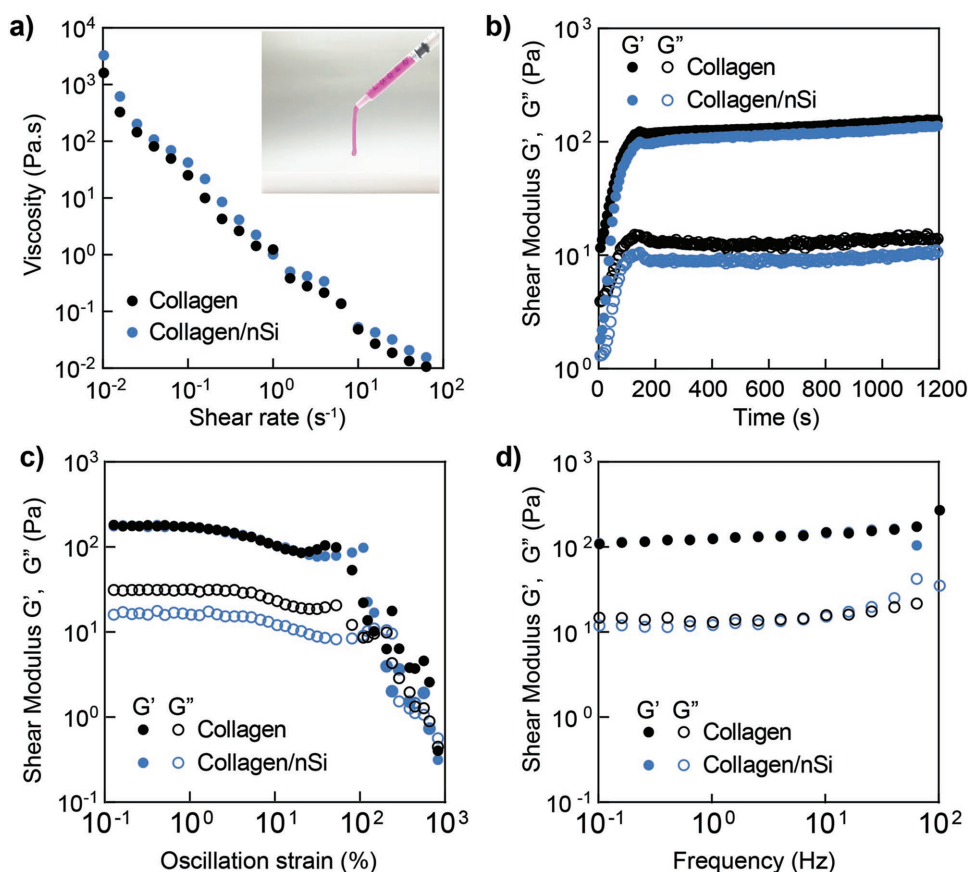


**Figure 3.** Rheological analysis for collagen and collagen/nanosilicates (nSi) hydrogels. Representative data (mean) shown for all data;  $n = 3$ . a) Shear-rate sweeps indicating shear-thinning behavior, b) temperature/time sweep indicating the curing of collagen hydrogels, c) amplitude sweep, and d) frequency sweep. All tests indicate that addition of nSi (0.015%) do not alter mechanical properties of collagen matrices.

quickly and are therefore homogeneously localized throughout the collagen matrix compared to growth factor that can freely diffuse through the matrix when no nanosilicates are present. Interestingly, blank nanosilicates loaded and mixed into the collagen matrices behave very similarly to pre-growth factor-loaded nanosilicates suggesting that when growth factor is administered exogenously and not immediately used sequestration may occur. Morphology of invading cells appears consistent throughout all samples (Figure 4a and 4b) because the collagen matrix predominately regulates cell morphology, while nanosilicates/growth factors are responsible for cell invasion.

### 2.5. Nanocomposites with Gradient of Proangiogenic Factors

Developing nanocomposite hydrogels with tailored functionality has opened up new possibilities in engineering advanced biomaterials for various biomedical and biotechnological applications.<sup>[34]</sup> Unfortunately, very few nanoparticles have been developed to influence cell migration and angiogenesis. Previously, a range of appropriate biological clues, such as VEGF, FGF, and PDGF have been incorporated within hydrogels to direct cell migration.<sup>[35]</sup> While effective, this incorporation strategy limits the time that growth factors are available since

they may freely diffuse throughout the matrix or solution, causing sprouting to occur at random locations. To establish that individual growth factors adsorb to nanosilicates surface and that there is a synergistic effect, a similar invasion assay is carried out with each growth factor individually and in combination (Figure 5). In all cases nanosilicates loaded with growth factors and embedded in 3D collagen matrices induced endothelial invasion (Figure 5a). Single growth factors produced a mild response with a relatively low number (<50) and low distance (<250  $\mu\text{m}$ ). Although PDGF has been well studied as an important growth factor during wound healing by promoting angiogenesis, the combination with nanosilicates did not produce as strong of a response as expected. There is a statistically significant ( $p < 0.001$ ) difference of combining PDGF with VEGF or FGF compared to PDGF by itself (Figure 5b,c). FGF and VEGF combinations resulted in little to no change when compared to combinations, except for the combination of all three growth factors. Results could be due to the short half-life of PDGF compared to FGF and VEGF, or the inability of PDGF to bind to nanosilicates. Overall, these results are consistent with the behavior of these growth factors in the literature<sup>[5,27,36]</sup> and confirm the ability of nanosilicates to deliver angiogenic factors in specific combinations and efficiencies to direct cellular invasion.

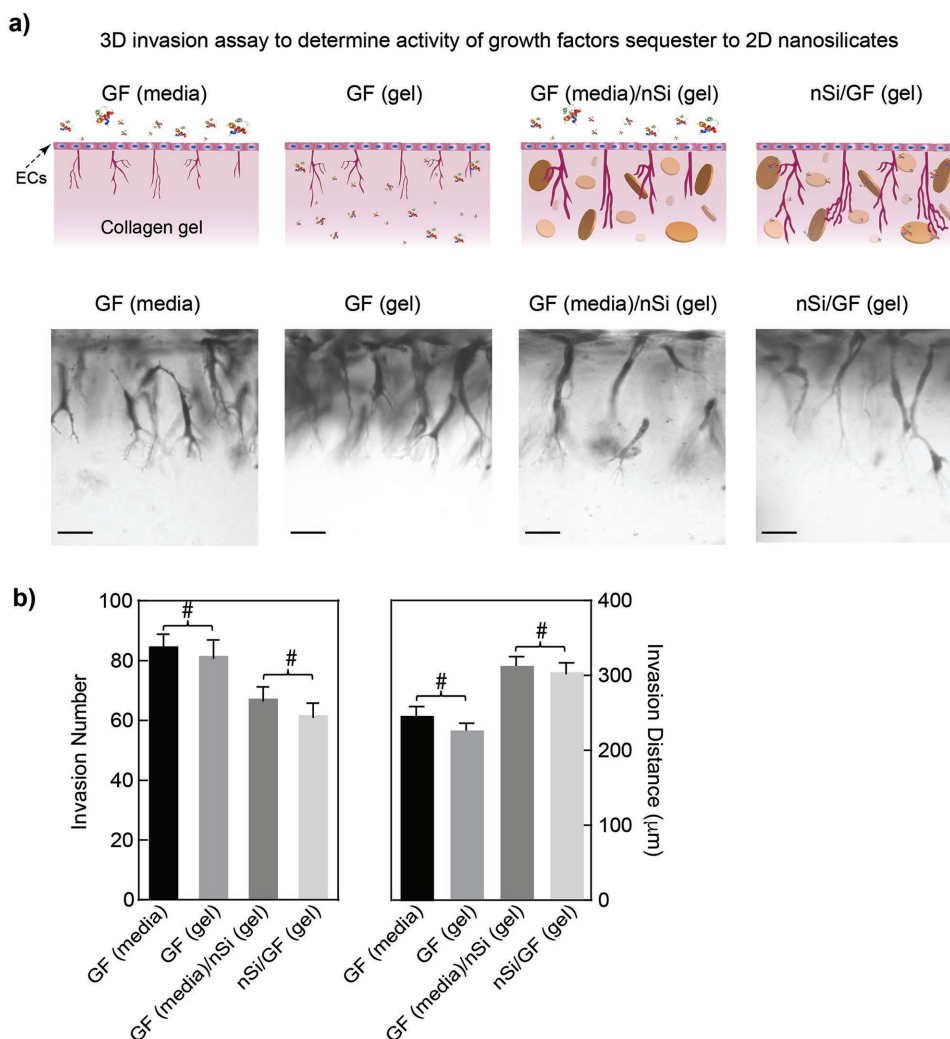


**Figure 4.** Nanosilicates incorporated into collagen matrices reduce invasion density but increase invasion distance. a) Schematic illustrating experimental conditions: growth factor in media (GF (media)), growth factor in collagen gel (GF (gel)), growth factor in media and nanosilicates in collagen gel (GF (media)/nSi (gel)), and growth factor and nanosilicates in collagen gel (nSi/GF (gel)). Photographs of invading structures (Scale bar = 50  $\mu\text{m}$ ) ( $n = 3$ , mean  $\pm$  standard deviation). b) Quantification of invading structures and invasion distance. Significance was determined using analysis of variance with Tukey's post hoc test for multiple comparisons and multiplicity-adjusted  $P$ -values. The symbol # denotes a significant relationship between the bracketed columns,  $p < 0.05$ .

## 2.6. Patterning Growth Factor-Sequester Nanosilicates

Tissues and interfaces within the human body display complex cellular and mechanical characteristics. Current approaches rely on discrete material steps with individual properties rather than continuous gradient designs.<sup>[37]</sup> Commonly, layered or stratified scaffolds often incorporate multiple materials and cell types to mimic the distinct tissue regions.<sup>[38]</sup> Alternatively, gradient scaffold designs can mimic the gradual change in the physical and mechanical properties that are present at the native tissue interface, and therefore offer a seamless transition between tissue regions without being susceptible to delamination.<sup>[39,40]</sup> Previous development of a facile approach to fabricate a nanocomposite gradient hydrogel using the material's flow properties has occurred.<sup>[39,41]</sup> As a culmination, we aim to fabricate injectable collagen-based scaffolds that can be patterned by the inclusion of specific growth factors. A 2 mm deep, 1 cm long well was

created on Teflon in which to inject various solutions. Collagen/nanosilicates matrices were injected into the well and allowed to flow through the channel (Figure 6a). Nanosilicate addition to collagen matrices does not change its flow properties (Figure 2a), and the flow is dependent on the time it takes the solution to polymerize. During the polymerization phase, there was sufficient time for two separate solutions to flow to the middle and form a complete matrix. The concentration of nanosilicates is constant throughout, but in one solution the nanosilicates were loaded with growth factors (FGF and VEGF), while the second contained pure collagen with no growth factor. Invasion of endothelial cells was observed on the end containing growth factors and not on the pure collagen/nanosilicates matrix (Figure 6b). Of note, there appears to be an increasing number of invading cells as the gradient progresses toward the end where growth factor-loaded nanosilicates were placed. This suggests that the two similar materials (difference being the inclusion of growth factor) mixed through

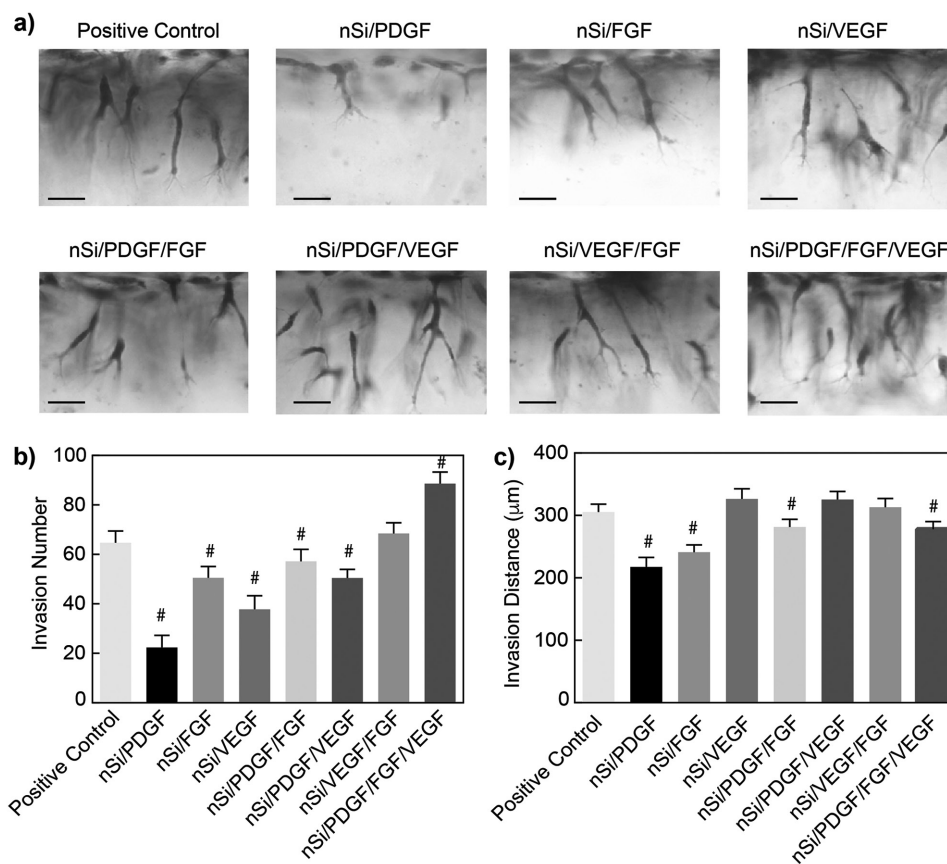


**Figure 5.** Nanosilicates deliver multiple GFs to enhance angiogenic responses. Nanosilicates (nSi) are loaded with PDGF, bFGF, VEGF alone, and in combination prior to embedding in collagen matrices. Positive control represents growth factors in media with blank nanosilicates in the gel (see Figure 4, condition 3 (GF(media)/nSi(gel))). a) Photographs of invasion responses (Scale bar = 50 µm), and quantification of b) invading structures and c) invasion distance ( $n = 3$ , mean  $\pm$  standard deviation). Significance was determined using analysis of variance with Tukey's post hoc test for multiple comparisons and multiplicity-adjusted  $P$ -values. The symbol # denotes a significant relationship between the indicated column and positive control,  $p < 0.03$ .

simple diffusion and flow through the channel. This facile approach demonstrates a method to pattern a gradient of endothelial cell ingrowth while maintaining mechanical properties. Potential applications are in tendon or ligament repair where there is a gradient of cells but no difference in matrix material properties. A simple unidirectional channel and nanosilicate/growth factor (combination) suggests that this concept can be furthered for precise localization of growth factor to generate more complex structures.

### 3. Conclusions

In summary, our results demonstrate the stability of nanosilicate/growth factor conjugates and their ability to deliver growth factors to induce an angiogenic response. The sequestration of growth factors permits greater depth penetration of invading cells, creating more fully formed more blood-vessel-like structures. We observe robust endothelial cell penetration into collagen matrices loaded with nanosilicates. The resulting invasions are controlled predominantly by the type of growth factors conjugated to the nanosilicates. Nanosilicates have been shown to have potential for delivering biomolecules;<sup>[19]</sup> however, this work is the first to show the importance

of nanoparticle-therapeutic conjugation for angiogenic potential through modulation of cell behaviors with important ramifications in the selection of growth factors and ability to investigate new therapeutics through use of a 3D cellular invasion assay.

### 4. Experimental Section

**Materials and Growth Factor Conjugation:** Laponite XLG (Nanosilicates, nSi) was obtained from Byk Additives and Instruments, dried in oven at 100 °C for 4 h prior to use, and mixed with ultrapure H<sub>2</sub>O. Growth factors were suspended within the nanoparticle solutions (40–400 ng mL<sup>-1</sup>), and solutions were allowed to rest overnight before being ultracentrifuged. Supernatant was removed and stored to use for invasion assay. The prepared media was used within 24 h after preparation. Alternatively, growth factor conjugated nanosilicate was suspended (0.005–0.015% w/v) in rat-tail collagen Type I was purified in the lab for invasion assays. Fetal bovine serum (FBS) was conjugated for 1 h and subsequent release was measured over a 48 h time period via microBCA Assay (ThermoFisher).

**Cell Culture:** Certified single-donor human umbilical vein endothelial cells (Lonza, Allendale, NJ) at passages 3–6 were cultured in 75 cm<sup>2</sup> flasks (Corning) coated with 1 mg mL<sup>-1</sup> sterile gelatin. Growth medium was previously described in detail<sup>[27]</sup> and consisted of M199, supplemented with FBS (15% v/v), bovine hypothalamic extract (0.04% w/v), heparin (0.01% w/v), antibiotics (1.2% v/v), and gentamycin (0.12% v/v).

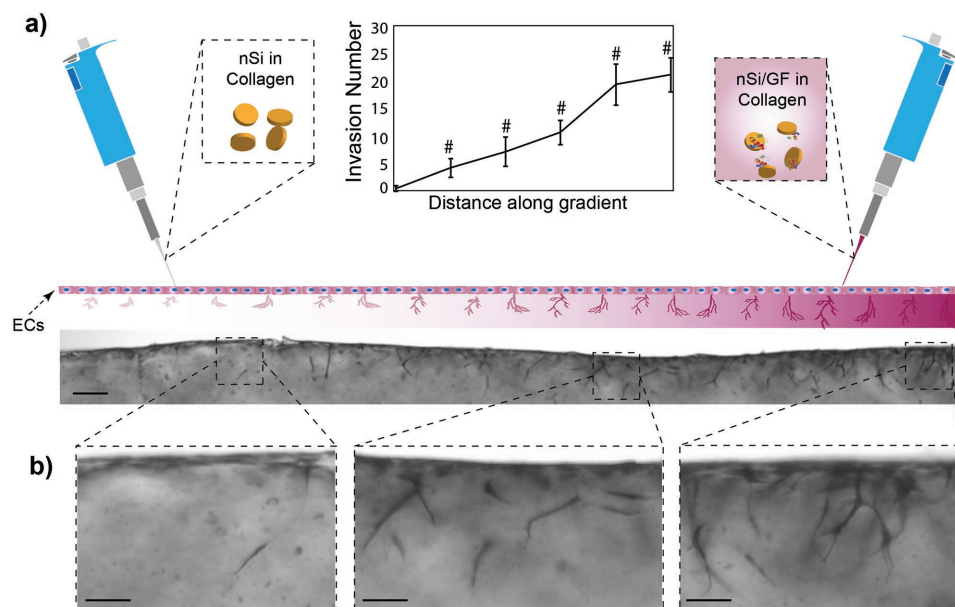


**Figure 6.** Nanosilicates offer the unique ability to pattern the delivery of growth factors. a) In this assay, nanosilicates (nSi) are incorporated into 3D collagen matrices as a gradient. The number of invading structures was quantified and averaged from three independent experiments. Data shown are average numbers of invading cells ( $n = 3$ , mean  $\pm$  standard deviation). b) Photograph of entire 8 mm gradient formed with blank nanosilicates and growth factor–loaded nanosilicates. Insets show enlarged view of indicated structures (Scale bar = 50  $\mu\text{m}$ ). Significance was determined using student's  $t$ -test to compare each point along gradient to previous point. The symbol # denotes a significant relationship between the indicated point and the point 1 step closer to origin,  $p < 0.05$ .

**Invasion Assay:** 3D invasion experiments were established using 2.5 mg mL<sup>-1</sup> type I collagen matrices containing  $1 \times 10^{-6}$  M S1P (Sigma, St Louis, MO). Confluent endothelial cell monolayers were seeded at 30 000 cells per well in M199 supplemented with  $1 \times \text{RSII}$  and in controls, 40 ng mL<sup>-1</sup> VEGF and bFGF. Where indicated, growth factors were incubated with multiple concentrations of Laponite (nanosilicates, nSi) for 1 h on ice. Laponite was then mixed into collagen matrices prior to plating in 96-well plate. After 24 h incubation at 37 °C with 5% CO<sub>2</sub>, invading cells were fixed with 3% glutaraldehyde in phosphate buffered saline and stained with 0.1% toluidine blue/30% methanol. Results from at least three independent experiments are shown.

**Quantification of Invasion Responses:** For invasion density measurements, a minimum of three fields were quantified manually as described.<sup>[27]</sup> Briefly, invasion density was quantified at 10x with an eyepiece containing a mounted reticle that displays a 10  $\times$  10 square grid. In the field of interest, the number of invading cells was recorded using a cell counter in a 2  $\times$  2 square area of the grid. For invasion distance, gels are sliced and laid on their side. Ten random photographs were taken at 4x magnification. The distance migrated from the monolayer was recorded using side view images taken with an Olympus CK-5 microscope with 150 or more structures from each treatment group were included in the analysis. A structure is the furthest tip of a migrating cell. Peripheral sprouts were not included. Image-Pro PLUS (MediaCybernetics, MD) software was used to quantify invasion distance.

**Dynamic Light Scattering and Zeta Potential Measurements:** DLS and zeta potential were measured on a Zetasizer Nano ZS (Malvern Instruments). One mL of nanosilicates or nanosilicates + fetal bovine serum (mixed for 1 h) was diluted 1:100 with phosphate buffered saline (PBS) and loaded into the instrument for both measurements. DLS samples were subsequently used for Zeta-potential samples and then discarded. Data were analyzed plotted and analyzed using Prism Graphpad 6.

**Mechanical Analysis:** A Discovery Hybrid Rheometer 2 (TA Instruments, New Castle, Delaware, USA) with attached 40 mm parallel plate at gap height of 0.1 mm and Peltier plate accessory was used for all experiments. Precursor solutions of collagen and collagen/0.05% nanosilicates (highest experimental concentration) were used for all experiments unless otherwise

noted. Rotational shear rate sweeps were executed between 10<sup>-2</sup> and 10<sup>2</sup> (s<sup>-1</sup>) to determine shear-thinning behavior of solutions. Rotational temperature–time sweep combination was executed to determine curing characteristics. First a temperature ramp of 5 °C min<sup>-1</sup> was carried out from 25 to 37 °C at 1% strain, 1 Hz. Subsequently a time sweep at 1% strain, 1 Hz was used to determine the amount of time for curing to occur. Oscillatory shear strain sweeps between 10<sup>-1</sup> and 10<sup>3</sup> performed at 1 Hz and frequency sweeps between 10<sup>0</sup> and 10<sup>2</sup> performed at 1% strain were conducted to monitor the linear viscoelastic region and determine yield strain.

**Statistical Analyses:** All statistical analyses were performed using Prism 6 (Graphpad Software, Inc.). For all experiments, at least three independent experiments were performed with  $n > 3$  replicate samples per experiment and data are presented mean  $\pm$  standard deviation. No statistical method was used to predetermine sample size. Unpaired Student's  $t$ -test was performed on data comparing two groups, assuming similar variance. One-way or two-way analysis of variance with Holm-Sidak or Tukey's post hoc test for multiple comparisons and multiplicity-adjusted  $P$ -values are reported. In all studies,  $P$ -values  $< 0.05$  were considered significant.

## Supporting Information

Supporting Information is available from the Wiley Online Library or from the author.

## Acknowledgements

D.W.H. and C.W.P. contributed equally to this work. The paper was written through contributions of all authors. All authors have given approval to the final version of the paper. Research reported in this publication was supported by the National Institute of Biomedical Imaging and Bioengineering (NIBIB) of the National Institutes of Health (NIH) under Award No. DP2 EB026265 and R03 EB02345 and the National Science Foundation (NSF) under Award No. CBET1705852. The content is solely



the responsibility of the authors and does not necessarily represent the official views of the National Institutes of Health. The authors would like to acknowledge help from Dr. Manish K. Jaiswal for transmission electron microscopy (TEM) image of nanoparticles.

## Conflict of Interest

The authors declare no conflict of interest.

## Keywords

2D nanomaterials, angiogenesis, hydrogels, nanocomposites, therapeutic delivery

Received: March 22, 2018

Revised: April 19, 2018

Published online: June 11, 2018

- [1] a) R. H. Adams, K. Alitalo, *Nat. Rev. Mol. Cell Biol.* **2007**, *8*, 464; b) R. Kalluri, *Nat. Rev. Cancer* **2003**, *3*, 422.
- [2] P. S. Briquez, L. E. Clegg, M. M. Martino, F. Mac Gabhann, J. A. Hubbell, *Nat. Rev. Mater.* **2016**, *1*, 15006.
- [3] a) J. K. Carrow, L. Cross, R. W. Reese, M. Jaiswal, C. Gregory, R. Kaunas, I. Singh, A. K. Gaharwar, *Proc. Natl. Acad. Sci. USA* **2018**, *115*, E3905; b) D. Chimene, D. L. Alge, A. K. Gaharwar, *Adv. Mater.* **2015**, *27*, 7261.
- [4] J. I. Dawson, J. M. Kanczler, X. B. Yang, G. S. Attard, R. O. Oreffo, *Adv. Mater.* **2011**, *23*, 3304.
- [5] K. J. Bayless, G. E. Davis, *Biochem. Biophys. Res. Commun.* **2003**, *312*, 903.
- [6] R. Cao, E. Brakenhielm, R. Pawliuk, D. Wariaro, M. J. Post, E. Wahlberg, P. Le Boulch, Y. Cao, *Nat. Med.* **2003**, *9*, 604.
- [7] a) J. Rouwkema, N. C. Rivron, C. A. van Blitterswijk, *Trends Biotechnol.* **2008**, *26*, 434; b) E. A. Phelps, A. J. Garcia, *Regener. Med.* **2009**, *4*, 65; c) E. C. Novosel, C. Kleinhans, P. J. Kluger, *Adv. Drug Delivery Rev.* **2011**, *63*, 300.
- [8] a) U. Hersel, C. Dahmen, H. Kessler, *Biomaterials* **2003**, *24*, 4385; b) D. N. Woolfson, Z. N. Mahmoud, *Chem. Soc. Rev.* **2010**, *39*, 3464.
- [9] a) K. A. Rieger, N. P. Birch, J. D. Schiffman, *J. Mater. Chem. B* **2013**, *1*, 4531; b) R. S. Balkawade, D. K. Mills, *FASEB J.* **2012**, *26*, 198; c) I. Kalashnikova, S. Das, S. Seal, *Nanomedicine* **2015**, *10*, 2593.
- [10] a) J. L. Cleland, E. T. Duenas, A. Park, A. Daugherty, J. Kahn, J. Kowalski, A. Cuthbertson, *J. Controlled Release* **2001**, *72*, 13; b) L. E. Freed, G. Vunjak-Novakovic, R. J. Biron, D. B. Eagles, D. C. Lesnoy, S. K. Barlow, R. Langer, *Biotechnology* **1994**, *12*, 689.
- [11] E. A. Silva, D. J. Mooney, *Biomaterials* **2010**, *31*, 1235.
- [12] C. R. Ozawa, A. Banfi, N. L. Glazer, G. Thurston, M. L. Springer, P. E. Kraft, D. M. McDonald, H. M. Blau, *J. Clin. Invest.* **2004**, *113*, 516.
- [13] a) L. M. Ellis, D. J. Hicklin, *Nat. Rev. Cancer* **2008**, *8*, 579; b) A. K. Olsson, A. Dimberg, J. Kreuger, L. Claesson-Welsh, *Nat. Rev. Mol. Cell Biol.* **2006**, *7*, 359.
- [14] a) J. R. Xavier, T. Thakur, P. Desai, M. K. Jaiswal, N. Sears, E. Cosgriff-Hernandez, R. Kaunas, A. K. Gaharwar, *ACS Nano* **2015**, *9*, 3109; b) D. W. Thompson, J. T. Butterworth, *J. Colloid Interface Sci.* **1992**, *151*, 236.
- [15] G. Lokhande, J. K. Carrow, T. Thakur, J. R. Xavier, M. Parani, K. J. Bayless, A. K. Gaharwar, *Acta Biomater.* **2018**, *70*, 35.
- [16] a) H. Jung, H.-M. Kim, Y. B. Choy, S.-J. Hwang, J.-H. Choy, *Appl. Clay Sci.* **2008**, *40*, 99; b) S. Wang, Y. Wu, R. Guo, Y. Huang, S. Wen, M. Shen, J. Wang, X. Shi, *Langmuir* **2013**, *29*, 5030.
- [17] D. M. Gibbs, C. R. Black, G. Hulsart-Billstrom, P. Shi, E. Scarpa, R. O. Oreffo, J. I. Dawson, *Biomaterials* **2016**, *99*, 16.
- [18] a) S. Xiao, R. Castro, D. Maciel, M. Goncalves, X. Shi, J. Rodrigues, H. Tomas, *Mater. Sci. Eng., C* **2016**, *60*, 348; b) M. Roozbahani, M. Kharaziha, R. Emadi, *Int. J. Pharm.* **2017**, *518*, 312; c) F. B. Zeynabad, R. Salehi, M. Mahkam, *Appl. Clay Sci.* **2017**, *141*, 23.
- [19] a) N. Golafshan, R. Rezahasani, M. Tarkesh Esfahani, M. Kharaziha, S. N. Khorasani, *Carbohydr. Polym.* **2017**, *176*, 392; b) J. I. Dawson, R. O. Oreffo, *Adv. Mater.* **2013**, *25*, 4069.
- [20] R. C. Sainson, J. Aoto, M. N. Nakatsu, M. Holderfield, E. Conn, E. Koller, C. C. Hughes, *FASEB J.* **2005**, *19*, 1027.
- [21] D. Kedrin, J. van Rheenen, L. Hernandez, J. Condeelis, J. E. Segall, *J. Mammary Gland Biol. Neoplasia* **2007**, *12*, 143.
- [22] W. Koh, R. D. Mahan, G. E. Davis, *J. Cell Sci.* **2008**, *121*, 989.
- [23] a) W. B. Saunders, B. L. Bohnsack, J. B. Faske, N. J. Anthis, K. J. Bayless, K. K. Hirschi, G. E. Davis, *J. Cell Biol.* **2006**, *175*, 179; b) A. N. Stratman, W. B. Saunders, A. Sacharidou, W. Koh, K. E. Fisher, D. C. Zawieja, M. J. Davis, G. E. Davis, *Blood* **2009**, *114*, 237.
- [24] S. C. Su, E. A. Mendoza, H. I. Kwak, K. J. Bayless, *Am. J. Physiol. Cell Physiol.* **2008**, *295*, C1215.
- [25] K. J. Bayless, H.-I. Kwak, S.-C. Su, *Nat. Protocols* **2009**, *4*, 1888.
- [26] B. Ruzicka, E. Zaccarelli, L. Zulian, R. Angelini, M. Sztucki, A. Moussaid, T. Narayanan, F. Sciortino, *Nat. Mater.* **2011**, *10*, 56.
- [27] K. J. Bayless, H. I. Kwak, S. C. Su, *Nat. Protoc.* **2009**, *4*, 1888.
- [28] C. L. Duran, R. Kaunas, K. J. Bayless, *Sphingosine-1-Phosphate: Methods and Protocols*, Springer, New York, NY **2018**, pp. 99–115.
- [29] a) S. Langlois, D. Gingras, R. Beliveau, *Blood* **2004**, *103*, 3020; b) S. Spiegel, S. Milstien, *Nat. Rev. Mol. Cell Biol.* **2003**, *4*, 397.
- [30] a) L. B. Jakeman, M. Armanini, H. S. Phillips, N. Ferrara, *Endocrinology* **1993**, *133*, 848; b) D. Shweiki, A. Itin, G. Neufeld, H. Gitay-Goren, E. Keshet, *J. Clin. Invest.* **1993**, *91*, 2235.
- [31] a) C. W. Peak, J. Stein, K. A. Gold, A. K. Gaharwar, *Langmuir* **2018**, *34*, 917; b) S. A. Wilson, L. M. Cross, C. W. Peak, A. K. Gaharwar, *ACS Appl. Mater. Interfaces* **2017**, *9*, 43449; c) D. Chimene, C. W. Peak, J. L. Gentry, J. K. Carrow, L. M. Cross, E. Mondragon, G. B. Cardoso, R. Kaunas, A. K. Gaharwar, *ACS Appl. Mater. Interfaces* **2018**, *10*, 9957.
- [32] A. K. Gaharwar, S. M. Mihaila, A. Swami, A. Patel, S. Sant, R. L. Reis, A. P. Marques, M. E. Gomes, A. Khademhosseini, *Adv. Mater.* **2013**, *25*, 3329.
- [33] F. Chowdhury, S. Na, D. Li, Y. C. Poh, T. S. Tanaka, F. Wang, N. Wang, *Nat. Mater.* **2010**, *9*, 82.
- [34] a) P. Keratitayanan, J. K. Carrow, A. K. Gaharwar, *Adv. Healthcare Mater.* **2015**, *4*, 1600; b) A. M. Lowman, T. D. Dziubla, P. Bures, N. A. Peppas, *Adv. Chem. Eng.* **2004**, *29*, 75.
- [35] a) J. K. Carrow, A. K. Gaharwar, *Macromol. Chem. Phys.* **2015**, *216*, 248; b) A. K. Gaharwar, N. A. Peppas, A. Khademhosseini, *Biotechnol. Bioeng.* **2014**, *111*, 441.
- [36] a) K. J. Bayless, G. E. Davis, *J. Biol. Chem.* **2004**, *279*, 11686; b) A. N. Stratman, A. E. Schwindt, K. M. Malotte, G. E. Davis, *Blood* **2010**, *116*, 4720.
- [37] M. Singh, C. Berkland, M. S. Detamore, *Tissue Eng., Part B* **2008**, *14*, 341.
- [38] L. Liverani, J. A. Roether, P. Noeaid, M. Trombetta, D. W. Schubert, A. R. Boccaccini, *Simple Fabrication Technique for Multilayered Stratified Composite Scaffolds Suitable for Interface Tissue Engineering*, Elsevier, Kidlington, Royaume-Uni **2012**.
- [39] L. M. Cross, A. Thakur, N. A. Jalili, M. Detamore, A. K. Gaharwar, *Acta Biomater.* **2016**, *42*, 2.
- [40] H. H. Lu, S. Thomopoulos, *Annu. Rev. Biomed. Eng.* **2013**, *15*, 201.
- [41] L. M. Cross, K. Shah, S. Palani, C. W. Peak, A. K. Gaharwar, *Nanomedicine (N. Y., NY, U. S.)* **2017**, <https://doi.org/10.1016/j.nano.2017.02.022>.